Adıyaman University Journal of Science
https://dergipark.org.tr/en/pub/adyujsci
DergiPark AKADEMİK
ISSN 2147-1630
e-ISSN 2146-586X

Synthesis and Optical Characterization of a Novel Benzofuran-Based Molecule: 3-Amino-2-Pinacolone Benzofuran

Adnan KURT[1,*], Murat KOCA[2]

[1]*Adiyaman University, Faculty of Science and Arts, Department of Chemistry, 02040, Adiyaman, Türkiye*
akurt@adiyaman.edu.tr, ORCID: 0000-0001-8516-6525
[2]*Adiyaman University, Faculty of Pharmacy, Dept. of Pharm. Chemistry, 02040, Adiyaman, Türkiye*
mkoca@adiyaman.edu.tr, ORCID: 0000-0002-9250-0293

Received: 24.10.2025 **Accepted:** 14.12.2025 **Published:** 31.12.2025

Abstract

In the present study, a novel benzofuran-based compound, 3-amino-2-pinacolone benzofuran (APBF), was synthesized in high yield via the aldol condensation of 2-hydroxybenzonitrile with 1-chloropinacolone in the presence of potassium carbonate and acetonitrile. The structure of APBF was confirmed by FTIR and ^{1}H, ^{13}C-NMR spectroscopic analyses, which clearly defined its spectral characteristics. The UV–Vis absorption properties of APBF were comprehensively investigated to elucidate its photophysical behavior. Intense absorption bands were observed corresponding to π→π* transitions within the conjugated benzofuran framework, while the red-shifted bands were attributed to n→π* transitions arising from the carbonyl and amino functional groups. The APBF molecule exhibited excellent optical transparency in the higher wavelength region. Some optical dispersion parameters, including the single-oscillator energy, dispersion energy, oscillator strength, and oscillator wavelength were determined from the dispersion analysis. The optical band gap was found to be 3.311 eV indicating potential suitability of APBF for electro-optical applications. The relatively low Urbach energy (0.035 eV) indicated a well-ordered molecular structure with minimal defect-induced disorder confirming the excellent optical quality of the present molecule.

* Corresponding Author DOI: 10.37094/adyujsci.1810288

Keywords: Benzofuran; Uv–vis spectroscopy; Optical properties; Dispersion parameters.

Benzofuran Temelli Yeni Bir Molekülün Sentezi ve Optik Karakterizasyonu: 3-Amino-2-Pinakolon Benzofuran

Öz

Bu çalışmada, yeni bir benzofuran yapılı bileşik olan 3-amino-2-pinakolon benzofuran (APBF) bileşiği, potasyum karbonat ve asetonitril varlığında 2-hidroksibenzonitril ile 1-kloropinakolonun aldol kondenzasyonu yoluyla yüksek verimle sentezlendi. FTIR ile ^{1}H ve ^{13}C-NMR spektroskopik analizleri, APBF bileşiğinin yapısını doğrulamış ve karakteristik spektral özelliklerini açık bir şekilde ortaya koymuştur. UV–Vis absorpsiyon özellikleri ayrıntılı olarak incelenmiş ve bileşiğin fotofiziksel davranışı aydınlatılmıştır. Gözlenen güçlü absorpsiyon bantlarının, konjuge benzofuran iskeletindeki $\pi\rightarrow\pi^*$ geçişlerinden kaynaklandığı; kırmızı dalga boyuna kaymış bantların ise karbonil ve amino fonksiyonel gruplarına ait $n\rightarrow\pi^*$ geçişlerinden kaynaklandığı belirlenmiştir. APBF molekülü, yüksek dalga boyu bölgesinde mükemmel optik geçirgenlik sergilemiştir. Dağılım analizlerinden osilatör enerjisi, dağılım enerjisi, osilatör şiddeti ve osilatör dalga boyu gibi optik dağılım parametreleri belirlenmiştir. Optik bant aralığı 3.311 eV olarak bulunmuş olup, APBF molekülünün elektro-optik uygulamalar için potansiyel bir aday olabileceğini göstermektedir. Ayrıca, nispeten düşük Urbach enerjisi (0.035 eV), kusur kaynaklı düzensizliklerin oldukça az olduğu, iyi düzenlenmiş bir moleküler yapıya işaret etmektedir ve mevcut molekülün yüksek optik kalitesini doğrulamaktadır.

Anahtar Kelimeler: Benzofuran; UV–Vis spektroskopisi; Optik özellikler; Dağılım parametreleri.

1. Introduction

Oxygen-containing heterocyclic compounds represent a significant class of organic molecules that are widely studied due to their broad range of chemical reactivity and physicochemical properties [1]. These compounds, characterized by the presence of at least one oxygen atom within a cyclic structure [2], include furan [3], chromone [4], coumarin [5], isocoumarin [6] and benzofuran derivatives [7, 8], among others. Their prevalence in natural products and pharmaceuticals has garnered substantial attention in the fields of medicinal chemistry, materials science, and synthetic organic chemistry [1, 9]. Their structural versatility allows for diverse functionalization, which, in turn, facilitates the modulation of their biological and physicochemical behavior. Additionally, many oxygenated heterocycles possess aromatic character, enabling π-conjugation and electron delocalization, features that are critically important

for the development of novel materials for optical, electronic, and biomedical applications [10]. Among these, benzofuran compounds hold a unique position due to their rigid planar structures and extensive π-conjugation [11]. Benzofurans have emerged as a valuable platform for the design of biologically active molecules [12-14], fluorescent probes [15], and organic semiconductors [16].

Structurally, the benzofuran nucleus consists of a fused bicyclic system composed of a benzene ring and a five-membered oxygen-containing furan ring [17]. This fused arrangement allows for significant π-electron delocalization across the entire system, contributing to both chemical stability and unique photophysical characteristics [18]. Substituents introduced on either the benzene or furan rings can further modulate electronic properties, leading to compounds with enhanced reactivity or tailored optoelectronic features [19, 20].

Various synthetic strategies have been developed to construct benzofuran scaffolds efficiently. Classical methods include the reaction of salicylaldehyde with ethylchloroacetate or with α-haloketones [7]. Recent advancements in transition metal-catalyzed reactions, such as the palladium-catalyzed reactions between phenols and olefins, have expanded the synthetic toolbox for benzofuran derivatives [21]. Moreover, green chemistry approaches utilizing microwave irradiation, ionic liquids, or solvent-free conditions have also been explored to enhance reaction efficiency and reduce environmental impact [22-24].

Benzofuran derivatives exhibit a broad spectrum of pharmacological activities, including antimicrobial, anti-inflammatory, antitumor, antiviral, and antioxidant effects [14]. Many natural and synthetic benzofurans function as enzyme inhibitors [14], receptor modulators [25], or DNA-interacting agents [26]. In medicinal chemistry, strategic functionalization of the benzofuran core has been employed to enhance target specificity, reduce toxicity and improve pharmacokinetics, underscoring the scaffold's significance in drug development [14, 27].

In addition to their biological relevance, benzofurans possess remarkable optical properties that make them suitable for optoelectronic applications. The extended π-conjugation in the benzofuran system contributes to strong absorption in the UV–visible region, making these compounds attractive candidates for use in organic light-emitting diodes (OLEDs) [28], photovoltaic cells [29], and nonlinear optical (NLO) materials [30]. Substitution at specific positions on the benzofuran scaffold can finely modulate electronic transitions [19], thereby facilitating intramolecular charge transfer [31] and improving fluorescence efficiency or photoresponsive behavior [15]. Furthermore, benzofuran derivatives have found widespread application in polymer science, particularly as monomeric units designed to enhance charge

mobility, thermal stability, and processability, which are critical factors for the development of advanced polymeric materials [32, 33].

Although several studies exist, the literature still lacks comprehensive work on the synthesis and property evaluation of functionally diverse benzofuran derivatives. To address this gap, the present study focuses on the optical properties of π-conjugated and functionally substituted benzofuran derivatives. In this context, we synthesized and spectrally characterized a new compound, 3-amino-2-pinacolone benzofuran (APBF), bearing both amino and ketone functional groups. The UV–Vis absorption characteristics of this compound were first investigated in detail to elucidate its photophysical behavior. These findings are expected to contribute to existing gaps in the literature related to the structure–property relationships of benzofuran derivatives. Notably, the synthesized molecule may exhibit features consistent with organic semiconductors, suggesting its potential utility in optoelectronic applications.

2. Materials and Methods

2.1. Materials

2-Hydroxybenzonitrile, 1-chloropinacolone, potassium carbonate, acetonitrile, tetrahydrofuran (THF) and ethyl alcohol were all purchased from Sigma-Aldrich.

2.2. Synthesis of 3-amino-2-pinacolone benzofuran

A novel benzofuran based compound, 3-amino-2-pinacolone benzofuran, was synthesized using the aldol condensation method of salicylnitrile and α-haloketones as reported in the literature [34]. For this purpose, 2-hydroxybenzonitrile (0.01 mol, 1.191 g), 1-chloropinacolone (0.01 mol, 1.341 g), and potassium carbonate (0.015 mol, 2.073 g) were added to a reaction flask containing acetonitrile (50 mL). The reaction mixture was refluxed with continuous stirring for 12 h. After completion, part of the solvent was evaporated, and the remaining mixture was poured into water to precipitate the product. The precipitate was filtered, washed with water, and dried. The crude product was recrystallized from ethyl alcohol to afford pure 3-amino-2-pinacolone benzofuran as a crystalline solid in 86% yield (mp 139 °C). Its synthesis is illustrated in Scheme1.

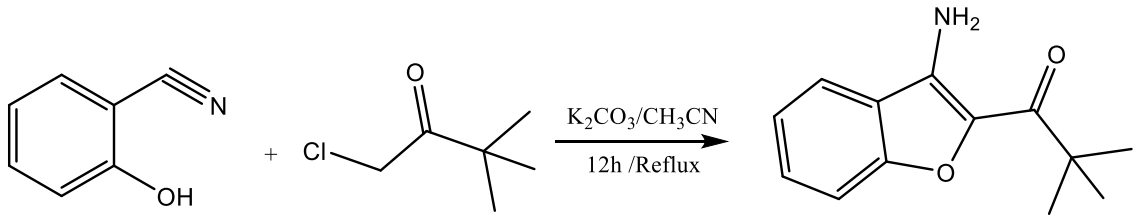

Scheme 1: Synthesis of 3-amino-2-pinacolone benzofuran (APBF) compound

2.3. Instrumental Techniques

FTIR spectra were recorded using a PerkinElmer Spectrum 100 FTIR spectrometer. 1H-NMR spectra were obtained on a Bruker Avance III HD spectrometer operating at 300 MHz, using deuterated chloroform ($CDCl_3$) as the solvent. The melting point was measured using a Stuart SMP20 Melting Point Apparatus. UV–Vis absorption spectra were measured on a Perkin Elmer Lambda 25 UV/VIS spectrophotometer in the wavelength range of 200–750 nm. A concentrated stock solution of the APBF compound was initially prepared at a concentration of 0.400 mM order to minimize potential errors associated with the weighing of small sample quantities. For this purpose, 0.0022 g of APBF was accurately weighed and subsequently dissolved in tetrahydrofuran (THF) using a 25 mL volumetric flask under ambient laboratory conditions. 2.5 mL of this stock solution was diluted with THF in a 10 mL volumetric flask to obtain a working solution with a final concentration of 0.1 mM. UV–Vis analyses were then performed using this final solution.

3. Results and Discussion

The FTIR spectrum of 3-amino-2-pinacolone benzofuran (Fig. 1) exhibits characteristic absorption bands consistent with its proposed structure. The two sharp to slightly broad peaks at 3436 and 3307 cm^{-1} correspond to the asymmetric and symmetric N–H stretching vibrations of the primary amine ($–NH_2$) group. A strong absorption band at 1629 cm^{-1} is assigned to the C=O stretching vibration of a ketone moiety. The bands observed in the 3185–3060 cm^{-1} region arise from aromatic =C–H stretching vibrations of the benzofuran ring, while those between 2973–2872 cm^{-1} correspond to aliphatic C–H stretching of the tert-butyl substituents. Additionally, the absorptions at 1605 cm^{-1} and 1592 cm^{-1} are attributed to C=C stretching vibrations of the furan and benzene rings, respectively. The distinct peak at 1167 cm^{-1} is due to C-O-C stretching.

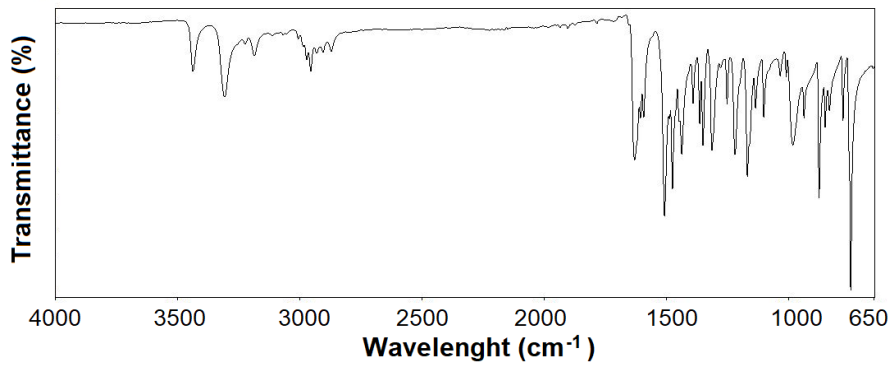

Figure 1: FTIR spectrum of 3-amino-2-pinacolone benzofuran (APBF) molecule

The structural characterization of the synthesized APBF compound was further confirmed by the ^{1}H-NMR spectrum, as presented in Fig. 2. The spectrum exhibited a singlet signal at 1.43 ppm, which was assigned to the methyl protons of the tert-butyl group. A singlet observed at 5.83 ppm was attributed to the amine (–NH_2) protons. The aromatic region displayed a multiplet between 7.20 and 7.62 ppm, corresponding to the aromatic protons of the benzofuran ring system. Additionally, the peak at 7.28 ppm arises from the residual $CDCl_3$ solvent. These spectral features are consistent with the expected structure of the synthesized compound.

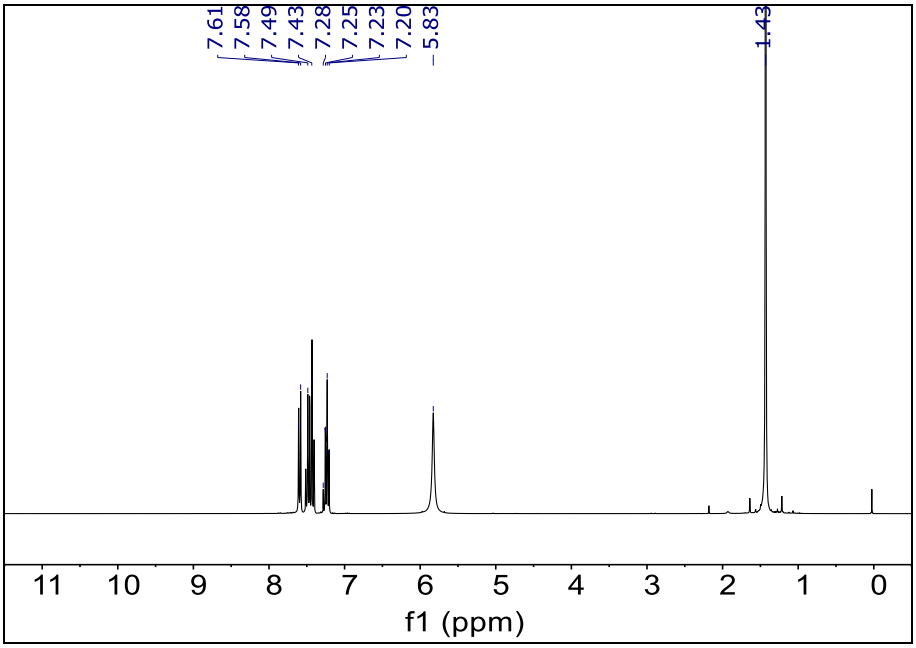

Figure 2: ^{1}H-NMR spectrum of the APBF molecule

For additional structural confirmation, ^{13}C-NMR spectroscopy was performed, and the resulting spectrum is presented in Fig. 3. The signal observed at 197.75 ppm corresponds to the ketone carbonyl carbon. The ipso carbon at 153.51 ppm is attributed to the carbon adjacent to the oxygen atom in the benzofuran ring, while the ipso carbon at 140.49 ppm is assigned to the carbon adjacent to the amine substituent. The series of peaks appearing between 134.39 and 112.49 ppm are characteristic of aromatic =CH carbons within the benzofuran framework, consistent with the expected six distinct aromatic carbons. The signal at 42.74 ppm is assigned to the ipso carbon of the tert-butyl group, and the three equivalent methyl carbons attached to this group resonate at 26.41 ppm. The signal at 77.53 ppm is for the residual $CDCl_3$ solvent.

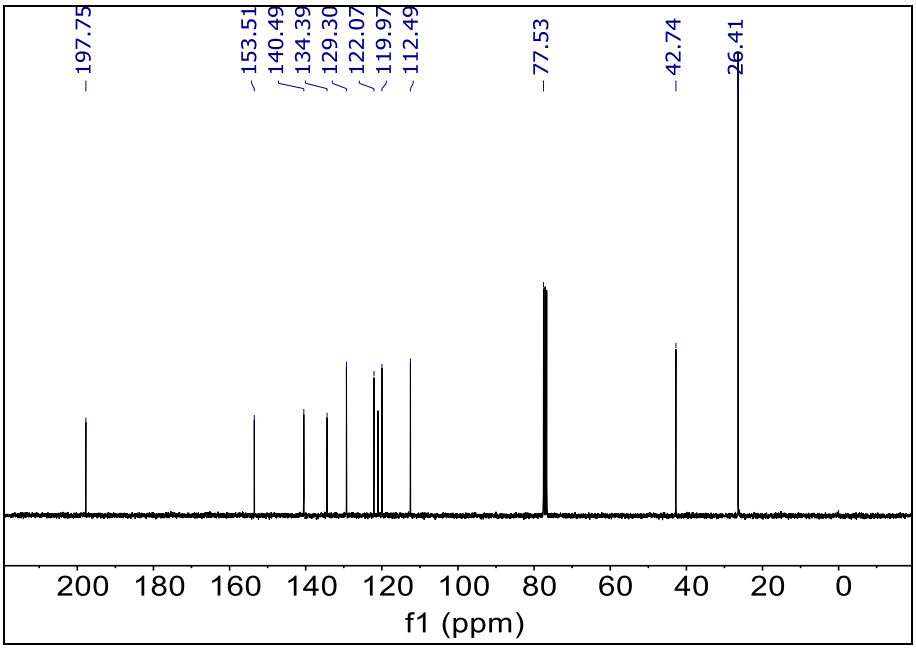

Figure 3: ^{13}C-NMR spectrum of the APBF molecule

The variation of transmittance (T) with wavelength for the APBF molecule is illustrated in Fig. 4. As seen from the figure, the transmittance exhibits three distinct minima within the examined spectral range. The first minimum appears at 255 nm with a transmittance of 14.48%, followed by a second at 305 nm with 10.85%. The lowest transmittance value, 6.95%, is observed at 345 nm. Beyond this wavelength, a sharp rise in transmittance occurs, reaching 99.97% at 395 nm. The transmittance value reaches its maximum transmittance of 99.99% at 450 nm and remains constant at this final value up to 750 nm. This steady plateau indicates that the APBF molecule exhibits excellent optical transparency in the higher wavelength region.

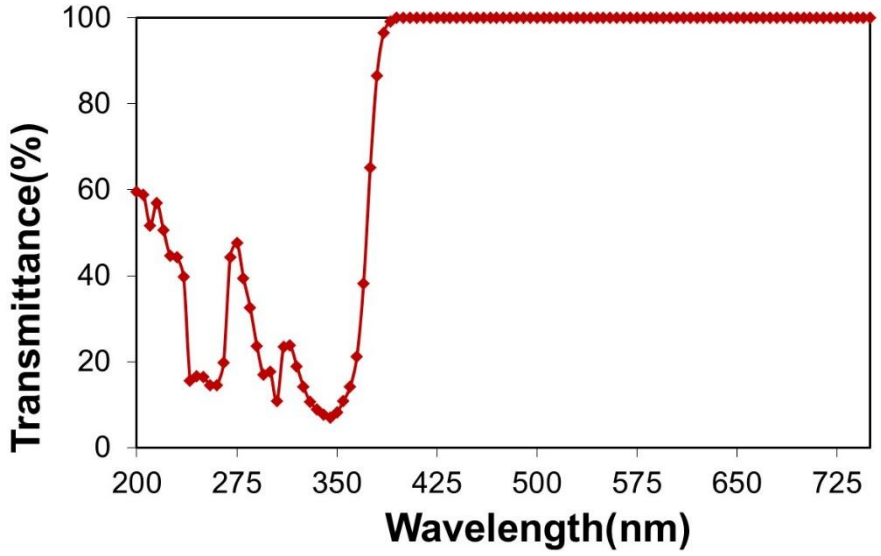

Figure 4: Transmittance measurements for the APBF molecule

Reflectance (R) is another important parameter in optical characterization and it can be calculated using the following equation between absorbance and transmittance values [35].

$$R = 1 - T - A \quad (1)$$

The reflectance spectrum of the APBF molecule (Fig. 5) demonstrates an inverse correlation with the corresponding transmittance data. The reflectance reaches its maximum intensity at wavelengths where transmittance is minimal and decreases sharply in regions where transmittance rises suddenly. A gradual reduction in reflectance is observed toward higher wavelengths, ultimately stabilizing at an approximately constant level within the 395–750 nm range. This behavior is consistent with typical optical responses of π-conjugated organic systems, where increased absorption at specific electronic transition regions leads to reduced reflectance [36].

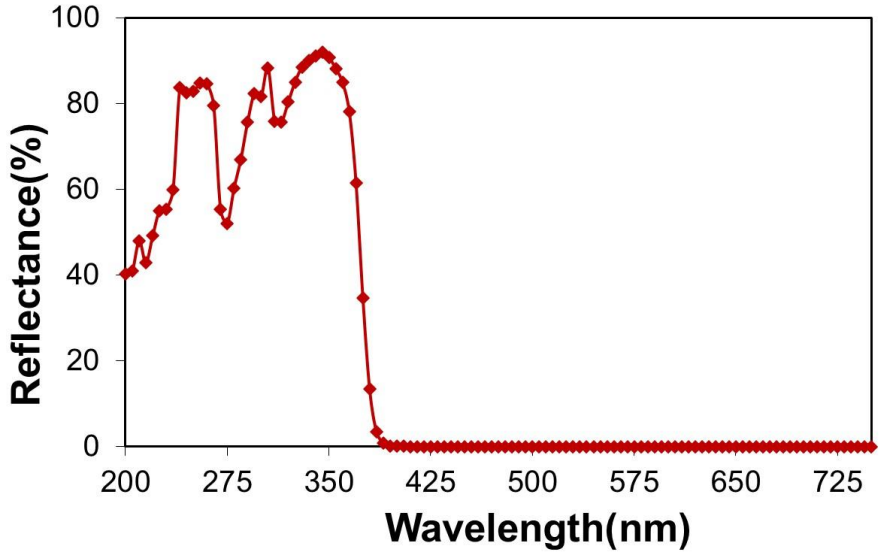

Figure 5: Reflectance measurements for the APBF molecule

In the UV–Vis spectrum of APBF, intense absorption bands are observed at lower wavelengths, corresponding to the π→π* transitions of the conjugated benzofuran framework. The red-shifted bands are typically attributed to n→π* transitions associated with the carbonyl and amino functional groups. The presence of both electron-donating (–NH_2) and electron-withdrawing (C=O) substituents within the π-conjugated benzofuran system facilitates intramolecular charge-transfer interactions, leading to a slight bathochromic shift and the appearance of a broad absorption tail extending toward 395 nm [37].

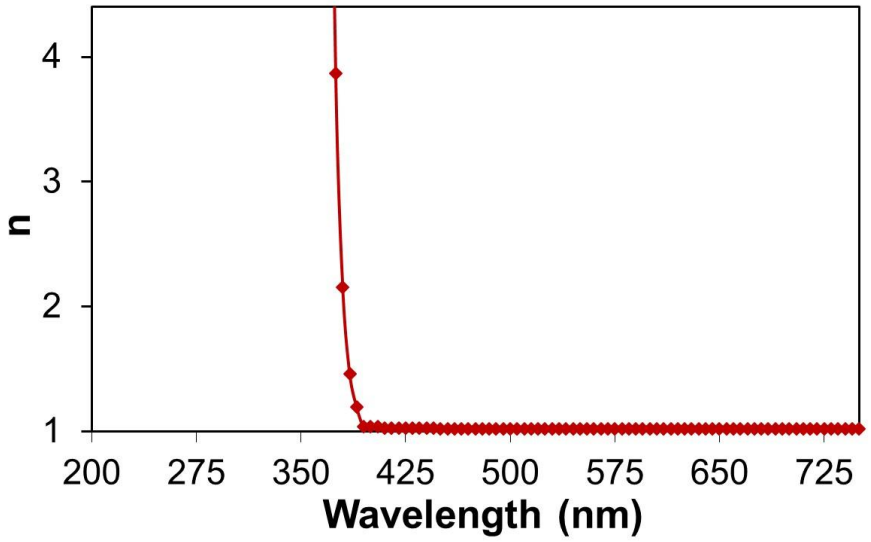

Figure 6: Variation of refractive index with wavelength of the APBF molecule

The refractive index (n) plays a crucial role in determining how light interacts with a material, influencing phenomena such as refraction, dispersion, and reflection. It also provides essential information about the wavelength-dependent optical behavior of the samples. In this study, the refractive index values were calculated using a simplified relation based on the reflectance and transmittance data obtained from UV–Vis spectroscopy measurements as given below [38]:

$$n = \left[\frac{1+R}{1-R}\right] - \sqrt{\frac{4R}{(1-R)^2} - k^2} \tag{2}$$

k is the extinction coefficient:

$$k = \frac{\alpha \lambda}{4 \pi} \tag{3}$$

α is the absorption coefficient:

$$\alpha = \frac{2.303\, A}{l} \tag{4}$$

where *l* denotes the optical path length of the sample cell. As shown in Fig. 6, the refractive index of the APBF molecule exhibits a distinct spectral dependence. At shorter wavelengths, higher refractive index values are observed, reflecting strong photon–electron coupling. With increasing wavelength, particularly beyond the resonance region at approximately 345 nm, the refractive index decreases sharply. This decline continues up to around 395 nm, after which the rate of decrease slows, reaching an almost constant value. Such wavelength-dependent refractive index

behavior is consistent with previously reported findings [39-44]. As an example, the refractive index was measured to be 3.87 at 375 nm and decreased to 1.02 at 750 nm.

Table 1. Optical results of APBF compound

E_g (eV)	E_u (eV)	E_0 (eV)	E_d (eV)
3.311	0.035	3.296	0.112
λ_0 (nm)	$S_0.10^{11}$ (m^{-2})	n (750 nm)	T% (750 nm)
368.3	2.5	1.02	99.99

The optical behavior of APBF molecule near its absorption edge was examined to gain insight into the nature of its electronic transitions. This analysis is crucial for understanding and optimizing the electro-optical characteristics of APBF, as it identifies the photon energy region where efficient absorption occurs. The optical band gap was estimated using the Tauc method, which relates the absorption coefficient (α) to the incident photon energy (hν) according to the following equation [45]:

$$(\alpha h\nu) = B\left(h\nu - E_g\right)^n \tag{5}$$

The exponent n characterizes the nature of the electronic transition. In the present work, a value of n=1/2 was employed to represent direct allowed transitions. A plot of $(\alpha h\nu)^2$ versus (hν) was constructed, as shown in Fig. 7, and extrapolation of the linear region to $(\alpha h\nu)^2 = 0$ provided the direct optical band gap (E_g) of APBF molecule, which was found to be 3.311 eV (Table 1). This value is consistent with other benzofuran derivatives and confirms the energy required for electronic excitation, providing insight into APBF's potential applications in electro-optical devices [19, 46, 47].

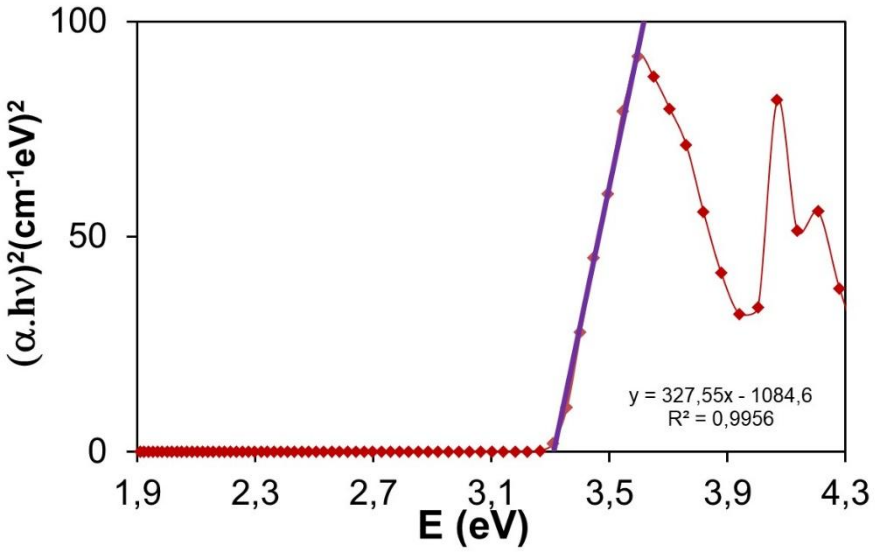

Figure 7: $(\alpha h\nu)^2$ vs. (E) plots of the APBF molecule

The Urbach energy (E_u) reflects the degree of exponential absorption near the optical band edge and is commonly associated with defect-related disorder and impurities that introduce localized states within the band gap. It quantifies the energetic width of these tail states adjacent to the band edges and thus serves as a reliable indicator of structural disorder in materials. It is derived from the exponential region of the absorption edge, where the absorption coefficient (α) exhibits a characteristic dependence on photon energy (E) according to the Urbach rule [48].

$$\alpha = \alpha_0 exp\left(\frac{E}{E_u}\right) \tag{6}$$

where α_0 is a specific constant. In the present study, the Urbach energy of the APBF compound was determined from the linear portion of the plot of ln(α) versus photon energy, as shown in Fig. 8. The calculated E_u value, listed in Table 1, represents the energetic width of the localized tail states near the band edge. The relatively low Urbach energy (0.035 eV) obtained for APBF compound indicates a well-ordered molecular structure with minimal defect-related disorder, confirming the good optical quality of the compound [49].

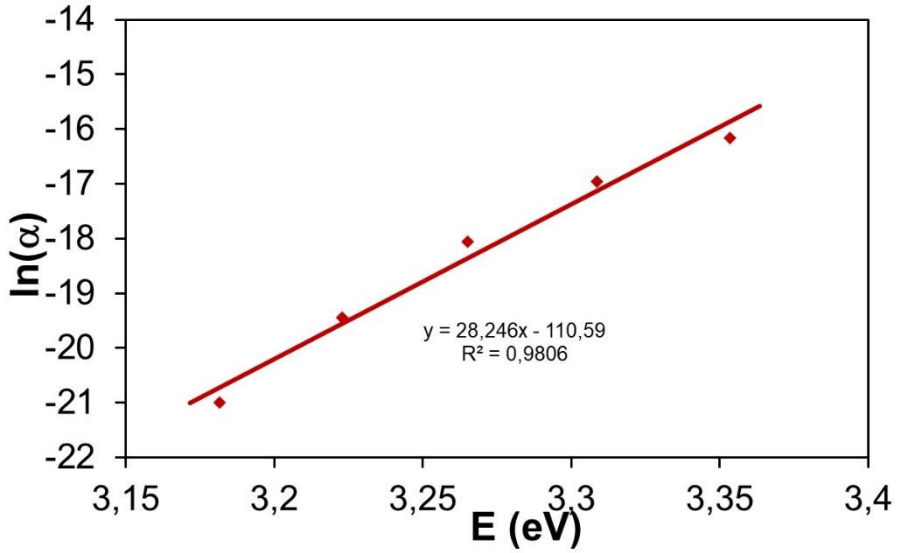

Figure 8. Dependence of ln(α) on E in the APBF molecule

The optical dispersion characteristics of materials are commonly described using the single-oscillator model proposed by Wemple and DiDomenico. This theoretical approach, based on interband electronic transitions, establishes a distinct relationship between the refractive index (n) and the photon energy (hν) through a characteristic dispersion expression [50, 51].

$$n^2(h\nu) = 1 + \frac{E_0\, E_d}{E_0^2 - (h\nu)^2} \tag{7}$$

The Wemple–DiDomenico single-oscillator model introduces two fundamental parameters: the single-oscillator energy (E_0), which represents the average energy of electronic transitions, and the dispersion energy (E_d), which reflects the strength of interband optical transitions. For practical evaluation, the model is presented in a linearized form, wherein plotting $(n^2 - 1)^{-1}$ against $(hv)^2$ produces a straight line. The slope and intercept of this plot correspond to $(E_0\, E_d)^{-1}$ and (E_0/E_d), respectively, allowing for the determination of both parameters, as illustrated in Fig. 9. For the APBF molecule, the calculated values of E_0 and E_d were found to be 3.296 eV and 0.112 eV, respectively, as listed in Table 1. As expected, the oscillator energy (E_0) is higher than the dispersion energy (E_d), since E_0 is associated with the average interband transition energy, while E_d is influenced by the localized electronic transitions [52]. The obtained results confirm that the electronic structure of APBF exhibits a well-defined dispersion behavior consistent with typical organic π-conjugated systems [43, 53].

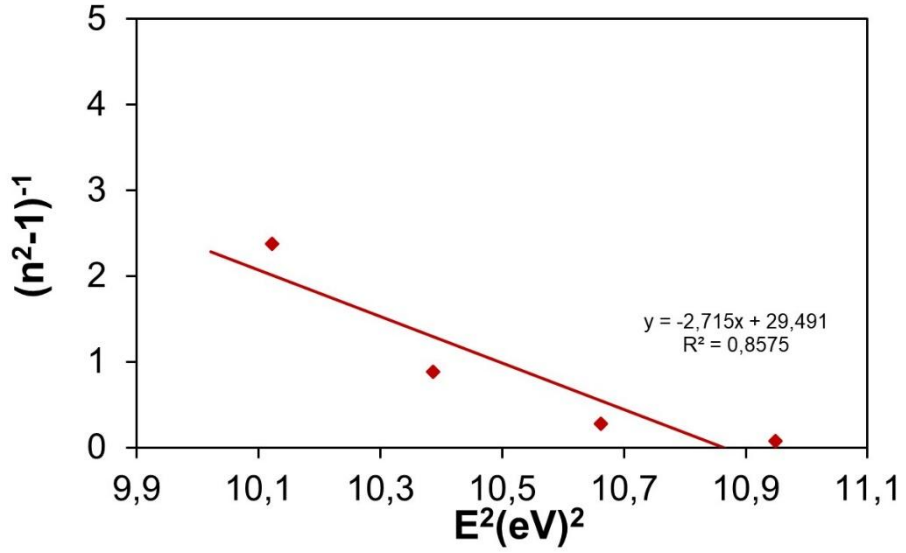

Figure 9. Variation of $(n^2\text{-}1)^{-1}$ with E^2 for the APBF molecule

The refractive index n(λ) of dielectric materials over a range of wavelengths is commonly described using the single-oscillator Sellmeier model. In this model, the optical dispersion characteristics are primarily governed by the oscillator strength (S_0) and the characteristic oscillator wavelength (λ_0), both of which are associated with electronic transitions. The single-term Sellmeier equation, widely employed to represent n(λ) across different wavelengths, thus provides a reliable framework for describing the dispersion behavior of dielectric and organic materials [54].

$$n^2(\lambda) - 1 = \frac{S_0 \lambda_0^2}{1 - (\lambda_0/\lambda)^2} \tag{9}$$

The parameter λ_0 represents the resonant wavelength associated with interband electronic transitions, while S_0 reflects the transition strength, incorporating factors such as polarizability and oscillator density. Together, these parameters provide a reliable description of the refractive index dispersion across the spectral range [43, 44, 53]. The single-oscillator parameters were determined by plotting $(n^2-1)^{-1}$ against λ^{-2}, where the slope and intercept of the resulting linear fit yielded the oscillator wavelength (λ_0) and oscillator strength (S_0), respectively. The corresponding plot is presented in Fig. 10, and the calculated values are summarized in Table 1. As observed, λ_0 was found to be 368.3 nm, while S_0 was determined to be 2.5×10^{11} m^{-2}.

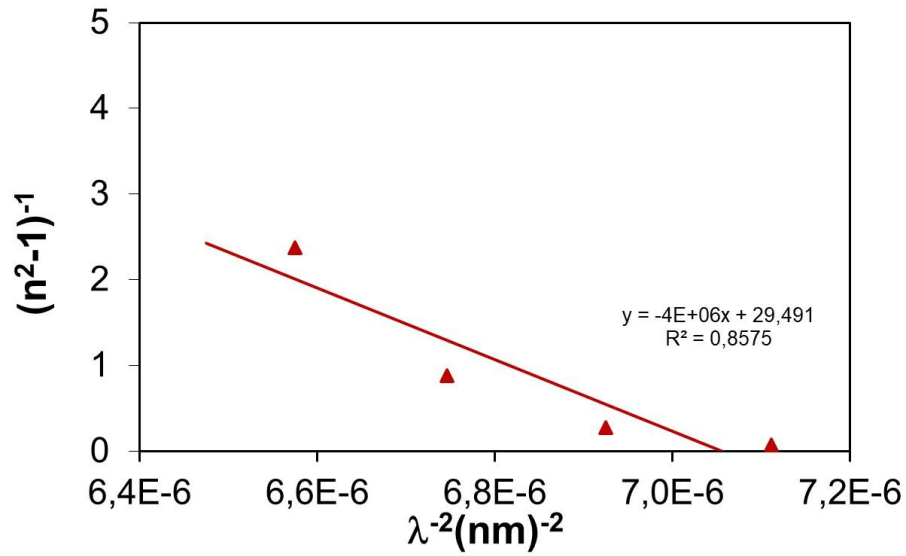

Figure 10. Relationship between $(n^2-1)^{-1}$ and $(\lambda)^{-2}$ for the APBF molecule

4. Conclusion

In this study, a new benzofuran-based compound, 3-amino-2-pinacolone benzofuran (APBF), was synthesized and structurally confirmed by FTIR, NMR and UV-vis spectroscopic analyses. The optical characterization revealed strong π→π* and n→π* transitions, consistent with its conjugated framework and functional groups. The optical band gap of APBF was determined as 3.311 eV, demonstrating its potential for electro-optical applications. Additionally, the low Urbach energy value of 0.035 eV reflected a highly ordered molecular arrangement with minimal structural disorder. These results collectively confirm the remarkable optical quality and promising photophysical properties of the synthesized APBF compound.

References

[1] Hillemane, V., Anil Kumar, N.V., *The oxygen-containing fused heterocyclic compounds*, IntechOpen, 2020, doi:10.5772/intechopen.88026.

[2] Currie, B.M., Neyt-Galetti, N.C., Olivier, T., Van der Merwe, P., Dibokwane, L.S., Reinhardt, A.M., et al., *Synthesis of an 8-membered oxygen-containing benzo-fused heterocycle using flow technologies – an exercise in undertaking research with sustainability as a driver*, RSC Sustainability, 3, 1356–1365, 2024.

[3] Izzotti, A., Pulliero, A., *The effects of environmental chemical carcinogens on the microRNA machinery*, International Journal of Hygiene and Environmental Health, 217, 601–627, 2014.

[4] Kanzouai, Y., Chalkha, M., Hadni, H., Laghmari, M., Bouzammit, R., Nakkabi, A., et al., , G., *Design, synthesis, in-vitro and in-silico studies of chromone-isoxazoline conjugates as anti-bacterial agents*, Journal of Molecular Structure, 1293, 136205, 2023.

[5] Kurt, A., Kaya, M., Koca, M., *Synthesis and characterization of coumarin derived surface active monomer*, Adıyaman University Journal of Science, 6, 110–121, 2016.

[6] Kurt, A., Avcı, H.İ., Koca, M., *Synthesis and characterization of a novel isocoumarin derived polymer and its thermal decomposition kinetics*, Macedonian Journal of Chemistry and Chemical Engineering, 37, 173–184, 2018.

[7] Mushtaq, A., Zahoor, A.F., Ahmad, S., Saif, M.J., Ul Haq, A., Khan, S.G., et al., *A comprehensive review on benzofuran synthesis featuring innovative and catalytic strategies*, ACS Omega, 9, 20728–20752, 2024.

[8] Koca, M., Kurt, A., Kırılmış, C., Aydoğdu, Y., *Synthesis, characterization and thermal degradation of novel poly(2-(5-bromo benzofuran-2-yl)-2-oxoethyl methacrylate)*, Polymer Engineering and Science, 52, 323–330, 2012.

[9] Dhameliya, T.M., Donga, H.A., Vaghela, P.V., Panchal, B.G., Sureja, D.K., Bodiwala, K.B., et al., *A decennary update on applications of metal nanoparticles (MNPs) in the synthesis of nitrogen- and oxygen-containing heterocyclic scaffolds*, RSC Advances, 10, 32740–32820, 2020.

[10] Borissov, A., Maurya, Y.K., Moshniaha, L., Wong, W.-S., Zyla-Karwowska, M., Stepien, M., *Recent advances in heterocyclic nanographenes and other polycyclic heteroaromatic compounds*, Chemical Reviews, 122, 565–788, 2022.

[11] Osati, S., Safari, N., Kalate Bojdi, M., Saeed Hosseiny Davarani, S., *Electrosynthesis of novel π-extended benzofuran derivatives of porphyrincatecholes*, Journal of Electroanalytical Chemistry, 655, 120–127, 2011.

[12] Yilmaz, A., Koca, M., Boga, M., Kurt, A., Ozturk, T., *Synthesis of novel oxime and benzofuran chemical frameworks possessing potent anticholinesterase activity: a SAR study related to Alzheimer disease*, ChemistrySelect, 8, e202302058, 2023.

[13] Yilmaz, A., Koca, M., Ercan, S., Acar, O.Ö., Boga, M., Sen, A., et al., *Amelioration potential of synthetic oxime chemical cores against multiple sclerosis and Alzheimer's diseases: evaluation in aspects of in silico and in vitro experiments*, Journal of Molecular Structure, 1318, 139193, 2024.

[14] Khanam, H., Shamsuzzaman, *Bioactive benzofuran derivatives: a review*, European Journal of Medicinal Chemistry, 97, 483–504, 2015.

[15] Krawczyk, P., *Modulation of benzofuran structure as a fluorescent probe to optimize linear and nonlinear optical properties and biological activities*, Journal of Molecular Modeling, 26, 272, 2020.

[16] Huang, P., Du, J., Biewer, M.C., Stefan, M.C., *Developments of furan and benzodifuran semiconductors for organic photovoltaics*, Journal of Materials Chemistry A, 3, 6244–6257, 2015.

[17] Patel, P., Vishakha, S.R., , Asati, V., Kurmi, B.D., Verma, S.K., Gupta, G.D., et al., *Furan and benzofuran derivatives as privileged scaffolds as anticancer agents: SAR and docking studies (2010 to till date)*, Journal of Molecular Structure, 1299, 137098, 2024.

[18] Mandado, M., Otero, N., Mosquera, R.A., *Local aromaticity study of heterocycles using n-center delocalization indices: the role of aromaticity on the relative stability of position isomers*, Tetrahedron, 62, 12204–12210, 2006.

[19] Kurt, A., Koca, M., *Optical properties of poly(2-(5-bromo benzofuran-2-yl)-2-oxoethyl methacrylate)/organoclay nanocomposites*, The Arabian Journal for Science and Engineering, 40, 2975–2984, 2015.

[20] Ibrahim, N., Moussallem, C., Allain, M., Segut, O., Gohier, F., Frère, P., *Exploring the electronic properties of extended benzofuran-cyanovinyl derivatives obtained from lignocellulosic and carbohydrate platforms raw materials*, ChemPlusChem, 86, 475–482, 2021.

[21] Sharma, U., Naveen, T., Maji, A., Manna, S., Maiti, D., *Palladium-catalyzed synthesis of benzofurans and coumarins from phenols and olefins*, Angewandte Chemie, 52, 12669–12673, 2013.

[22] Devi, A.P., Dhingra, N., Chundawat, R.S., Ameta, K.L., *Green synthesis of 2-benzylidene-1-benzofuran-3-ones and in vitro neuraminidase study using molecular docking*, SAR and QSAR in Environmental Research, 33, 499–512, 2022.

[23] Gopinathan, A., Aneeja, T.A., Abdulla, A.C.M., *Recent advances in the microwave assisted synthesis of benzofuran and indole derivatives*, Heterocycles, 103, 65, 2021.

[24] Sharifi, A., Abaee, M.S., Tavakkoli, A., et al., *An efficient and general procedure for room-temperature synthesis of benzofurans under solvent-free conditions using KF/Al2O3*, Journal of the Iranian Chemical Society, 5, S113–S117, 2008.

[25] Leow, M.L., Chin, H.L., Yu, P.S., Pasunooti, K.K., Tay, R.X., Zhang, D., et al., *Benzofuran-based estrogen receptor α modulators as anti-cancer therapeutics: in silico and experimental studies*, Current Medicinal Chemistry, 20, 2820–2837, 2013.

[26] Abdelhafez, O.M., Abedelatif, N.A., Badria, F.A., *DNA binding, antiviral activities and cytotoxicity of new furochromone and benzofuran derivatives*, Archives of Pharmacal Research, 34, 1623–1632, 2011.

[27] Khodarahmi, G., Asadi, P., Hassanzadeh, F., Khodarahmi, E., *Benzofuran as a promising scaffold for the synthesis of antimicrobial and antibreast cancer agents: a review*, Journal of Research in Medical Sciences, 20, 1094–1104, 2015.

[28] Shi, M., He, Y., Sun, Y., Fang, D., Miao, J., Ali, M.U., et al., *Bis(diphenylamino)-benzo[4,5]thieno[3,2-b]benzofuran as hole transport material for highly efficient RGB organic light-emitting diodes with low efficiency roll-off and long lifetime*, Organic Electronics, 84, 105793, 2020.

[29] Gao, Y., Saparbaev, A., Zhang, Y., Yang, R., Guo, F., Yang, Y., et al., *Efficient polymer solar cells based on poly(thieno[2,3-f]benzofuran-co-thienopyrroledione) with a high open circuit voltage exceeding 1 V*, Dyes and Pigments, 146, 543–550, 2017.

[30] Deng, G., Xu, H., Huang, H., Jiang, J., Kun, J., Zhang, X., et al., *Synthesis and properties study of a novel nonlinear optical chromophore containing benzo[b]furan moiety based on julolidine*, Journal of Molecular Structure, 1196, 439–443, 2019.

[31] Calikyilmaz, E., Karaoglu, G., Demir, M., Şahin, O., Ulgut, B., Akdag, A., et al., *Intramolecular through-space charge transfer between benzofuran and ynone groups on a naphthalene spacer*, Chemical Communications, 60, 550–553, 2024.

[32] Kurt, A., Yılmaz, P., *Thermal decomposition kinetics of benzofuran derived polymer/organosilicate nanocomposites*, Kuwait Journal of Science, 43, 172–184, 2016.

[33] Wang, D., Dou, K., Cui, W., Li, F., Jing, X., Yu, L., et al., *VOC enhancement of thienobenzofuran and benzotriazole backboned photovoltaic polymer by side chain sulfuration or fluoridation*, Dyes and Pigments, 184, 108775, 2021.

[34] Trofimov, F.A., Lelyak, G.F., Shevchenko, L.I., Grinev, A.N., *Condensation of salicylnitrile with some α-halo carbonyl compounds*, Chemistry of Heterocyclic Compounds, 10, 1016–1018, 1974.

[35] Nadeem, M.Y., Ahmed, W., *Optical properties of ZnS thin films*, Turkish Journal of Physics, 24, 651–659, 2000.

[36] Nosidlak, N., Dulian, P., Mierzwiński, D., Jaglarz, J., *The determination of the electronic parameters of thin amorphous organic films by ellipsometric and spectrophotometric study*, Coatings, 10, 980, 2020.

[37] Jung, J., Dinescu, A., *Emission pathway switching by solvent polarity: facile synthesis of benzofuran-bipyridine derivatives and turn-on fluorescence probe for zinc ions*, Tetrahedron Letters, 58, 358–361, 2017.

[38] Zidan, H.M., Abu-Elnader, M., *Structural and optical properties of pure PMMA and metal chloride-doped PMMA films*, Physica B: Condensed Matter, 355, 308–317, 2005.

[39] Kurt, A., *Influence of $AlCl_3$ on the optical properties of new synthesized 3-armed poly(methyl methacrylate) films*, Turkish Journal of Chemistry, 34, 67–69, 2010.

[40] Kurt, A., Koca, M., *Blending of poly(ethyl methacrylate) with poly(2-hydroxy-3-phenoxypropyl methacrylate): thermal and optical properties*, The Arabian Journal for Science and Engineering, 39, 5413–5420, 2014.

[41] Watanabe, I., Morikawa, K., Samitsu, S., Mori, H., *High refractive index copolymers from aromatic heterocycle-based vinyl sulfides and phthalimide/maleimide derivatives*, Macromolecular Chemistry and Physics, 224, 2300289, 2023.

[42] Fu, M.-C., Ueda, M., Ando, S., Higashihara, T., *Development of novel triazine-based poly(phenylene sulfide)s with high refractive index and low birefringence*, ACS Omega, 5, 5134–5141, 2020.

[43] Koca, M., Kurt, A., *Investigation of optical properties of a novel pyrazole containing polymer poly(1,3-diphenyl-1H-pyrazol-5-yl methacrylate) thin film*, Russian Journal of Physical Chemistry A, 96, 2967–2973, 2022.

[44] Kurt, A., Koca, M., *Blending of poly(methyl methacrylate) with poly(1,3-diphenyl-1H-pyrazol-5-yl methacrylate): investigation of its optical properties*, Adıyaman University Journal of Science, 12, 177–192, 2022.

[45] Tauc, J., *Optical properties of non-crystalline solids*, in: F. Abeles (Ed.), Optical Properties of Solids, North-Holland, Amsterdam, 1972, 277–313.

[46] Koca, M., Dagdelen, F., Aydoğdu, Y., *Thermal and optical properties of benzofuran-2-yl 3-phenyl-3-methylcyclobutyl thiosemicarbazone*, Materials Letters, 58, 2901–2905, 2004.

[47] Abdo, J., Ayoub, A., Ibrahim, N., Allain, M., Frère, P., *Tuning the solid state luminescence of benzofuran-cyanostilbenes by functionalization with electron donors or acceptors*, ChemPlusChem, 88, e202300402, 2023.

[48] Urbach, F., *The long-wavelength edge of photographic sensitivity and of the electronic absorption of solids*, Physical Review, 92, 1324–1324, 1953.

[49] Zhang, C., Mahadevan, S., Yuan, J., Ho, J.K.W., Gao, Y., Liu, W., et al., *Unraveling Urbach tail effects in high-performance organic photovoltaics: dynamic vs static disorder*, ACS Energy Letters, 7, 1971–1979, 2022.

[50] Wemple, S.H., DiDomenico, M., *Behavior of the electronic dielectric constant in covalent and ionic materials*, Physical Review B, 3, 1338–1351, 1971.

[51] Wemple, S.H., *Refractive-index behavior of amorphous semiconductors and glasses*, Physical Review B, 7, 3767–3777, 1973.

52] Veena, G., Lobo, B., *Dispersive parameters of oxidized PVA-PVP blend films*, Turkish Journal of Physics, 43, 337–354, 2019.

[53] El-Ghamaz, N.A., Ghoneim, M.M., El-Sonbati, A.Z., Diab, M.A., El-Bindary, A.A., Abd El-Kader, M.K., *Synthesis and optical properties studies of antipyrine derivatives thin films*, Journal of Saudi Chemical Society, 21, S339–S348, 2017.

[54] Wemple, S.H., DiDomenico, M., *Oxygen-octahedra ferroelectrics. I. Theory of electro-optical and nonlinear optical effects*, Journal of Applied Physics, 40, 720–734, 1969.